The RNA-Binding Region of Human TRBP Interacts with MicroRNA precursors via Two Independent Domains

Matthieu P. M. H. Benoit, Lionel Imbert, Andrés Palencia, Julien Pérard, Christine Ebel, Jérôme Boisbouvier and Michael J. Plevin*

Supplementary Information

Multi-signal analysis of SvAUC data.

Sedimentation profiles were obtained using three optical signals and were analyzed simultaneously with the program SEDPHAT (1) using a hybrid model of one non-interacting species (for either TRBP-D12 or pre-miR-155) and c(*s*) distributions representing minor species (e.g. an RNA dimer). Data sets concerning TRBP-D12 and pre-miR-155 were analysed separately.

The extinction coefficient at 280 nm for TRBP-D12 (10,084 cm^{-1} mol^{-1}) was fixed in order to derive an extinction coefficient at 260 nm (5,814 cm^{-1} mol^{-1}) and the fringe shift (ΔJ) increment (57,569 fringe cm^{-1} mol^{-1}) from the peak integrals. The extinction coefficient at 260 nm for pre-miR-155 (490,000 cm^{-1} mol^{-1}) was fixed in order to allow the extinction coefficient at 280 nm (225,975 cm^{-1} mol^{-1}) and the fringe shift increment (69,347 fringe cm^{-1} mol^{-1}) to be derived. Integration of the fast peak of the c(*s*) curves was used to determine the experimental ratios for the fast boundary.

Comparison of ITC binding models

ITC experiments in which pre-miR-155 was titrated into TRBP-D12 suggested the formation of complex in which more than one molecule of TRBP-D12 can bind pre-miR-155 (see below). Titrations of RNA samples (either pre-miR-155 or miR-155/miR-155*) with TRBP-D12 were consequently analysed using different models, including examples with successive binding of multiple molecules of TRBP-D12 to each miR-155 precursor. Only two protein/RNA interaction models could be reliably fitted to these data: a simple 1:1 model and a successive binding model with 2:1 stoichiometry. These two models are compared using Akaike weights (2, 3) and RMSDs in the table below. Both Akaike weights and RMSDs show that models in which two molecules of protein bind successively to a single molecule of RNA (either pre-miR-155 or miR-155/miR-155*) best explain the experiment data.

System	Stoichiometry		RMSD (kcal/mol)	Akaike weights
	Protein	RNA		
TRBP-D12 + pre-miR-155	1	1	0.13	1×10^{-28}
TRBP-D12 + pre-miR-155	2	1	0.05	$\simeq 1$
TRBP-D12 + miR-155/miR-155*	1	1	0.14	1×10^{-31}
TRBP-D12 + miR-155/miR-155*	2	1	0.04	$\simeq 1$

ITC experiments performed using single dsRBD constructs (e.g. TRBP-D1 and TRBP-D2) yielded binding isotherms with a single visible step, which were best described by a complex stoichiometry of 4 protein molecules per RNA. These data do not provide sufficient constraints to allow the fitting of the 4 microscopic binding constants and

enthalpies. Therefore, a single-site model was used to analyze these data. While a single-site model is not strictly appropriate for describing such interactions, it does permit a global comparison of the binding parameters that describe the interaction between the three TRBP constructs and pre-miR-155.

Modelling of the TRBP-D12/miRNA precursor complex

The 3D model of pre-miR-155 presented in Supplementary Figure 6 was generated using Rosetta (4). The 61-nucleotide sequence of pre-miR-155 (including the modifications made to the native sequence described) was split into three regions: two from the double stranded stem (region 1: 1-11 and 49-61; and region 2: 9-22 and 40-51) and one encompassing the apical loop (region 3: 19-43). Ensembles of 20 structures of the 3 fragments were generated using Rosetta (http://rosettaserver.graylab.jhu.edu). A pair-wise structural superposition of overlapping sequences was performed using ProFit (www.bioinf.org.uk/software/profit/index.html). Each aligned pair of structures were ranked. In each instance the structure from region 2 was defined as the template. A single 3D model of pre-miR-155 was constructed by combining aligned pairs of fragments with the same central region (region 2) with the lowest combined rank.

The model of the interaction between dsRBDs and pre-miR-155 was generated using the structure of TRBP-D2 in complex with a short 10 bp dsRNA (PDB code: 3ADL; (5)). The RNA fragment in 3ADL was extended by adding a symmetry-related dsRNA molecule to generate a 20 bp broken dsRNA fragment. The 20 bp dsRNA in the modified 3ADL was structurally aligned to the Rosetta model of pre-miR-155 using ProFit. The superposition was only performed for carbon atoms in the ribose ring of the template and mobile structures over a 16 bp window. This alignment process generated a model with a dsRBD molecule located at a potential binding site on the surface of pre-miR-155. The alignment was repeated by incrementing the starting position of the alignment window along the pre-miR-155 sequence to generate 28 models with a rmsd for like ribose atoms of less than 4.5 Å. A relatively high cut-off was selected to take account of the presence non-base-paired nucleotides (12, 16 and 37) and non-Watson Crick base pairing (21 and 41; and 24 and 38) in certain alignment windows.

Whilst clearly theoretical, this model does suggest that it is feasible for 4 dsRBDs to interact with both pre-miR-155 and miR-155/miR-155* without protein-protein contact.

Supplementary References

1. Balbo,A., Minor,K.H., Velikovsky,C.A., Mariuzza,R.A., Peterson,C.B. and Schuck,P. (2005) Studying multiprotein complexes by multisignal sedimentation velocity analytical ultracentrifugation. *Proc. Natl. Acad. Sci. U.S.A.*, **102**, 81–86.

2. Akaike,H. (1973) A new look at statistical model identification. *IEEE Transactions on Automatic Control*, **19**, 716–723.

3. Burnham,K.P. and Anderson,D.R. (2004) Model Selection and Multimodel Inference: A Practical Information-Theoretic Approach 2nd ed. Springer.

4. Das,R., Karanicolas,J. and Baker,D. (2010) Atomic accuracy in predicting and designing noncanonical RNA structure. *Nat. Methods*, **7**, 291–294.

5. Yang,S.W., Chen,H.-Y., Yang,J., Machida,S., Chua,N.-H. and Yuan,Y.A. (2010) Structure of Arabidopsis HYPONASTIC LEAVES1 and its molecular implications for miRNA processing. *Structure*, **18**, 594–605.

Supplementary Figure Legends

Supplementary Figure S1. Comparison of NMR data collected on different constructs of apo-TRBP. 2D (^{1}H,^{15}N) spectra of (a) apo-TRBP-D1 in red, (b) apo-TRBP-D2 in green, and (c) apo-TRBP-D12 black. A colored graphical representation of each construct is provided above the spectrum. (d) superposition of the spectra shown in (a-c) retaining the same color scheme and construct graphics. The spectrum of apo-TRBP-D12 can be readily recapitulated by superposing spectra of apo-TRBP-D1 and apo-TRBP-D2. Additional peaks not present in the red and green spectra originate from residues found in the interdomain linker in TRBP-D12. (e) Compound chemical shift differences between respective sites in single (either TBRP-D1 or TRBP-D2) and double domain (i.e. TRBP-D12) constructs plotted as a function of residue number. The large deviation seen at the C-terminus of TRBP-D1 is due to the presence of the inter-domain linker in TRBP-D12.

Supplementary Figure S2. Site-by-site comparison of the (^{1}H,^{15}N) chemical shift of a residue in the single domain and the corresponding residue in TRBP-D12. Circles denote (^{15}N) chemical shifts and squares (^{1}H) chemical shifts. Rmsd values for ^{1}H and ^{15}N chemical shifts are provided.

Supplementary Figure S3. Examples of the changes observed in peak position following the titration of TRBP-D12 with pre-miR-155. Regions of the spectra corresponding to L51, H58 and H85 from the first dsRBD, and R189, T208 and K211 from the second dsRBD are shown. The spectra are colored according the to RNA/protein ratio as defined in the inset.

Supplementary Figure S4. ITC analysis of the interaction between pre-miR-155 and single or double domain constructs. Examples of ITC data recorded when pre-miR-155 was titrated into (a) TRBP-D12, (b) TRBP-D1 and (c) TRBP-D2 constructs. Top panels show power *vs.* time. A schematic representation of the macromolecules in the sample is provided. The bottom panels show the integrated injection enthalpy per mole of injectant plotted as a function of the ratio of the protein and pre-miR-155 concentrations. The fit of each titration curve to a single-site binding model is shown by a solid red line. The parameters calculated for each fit are provided in the Supplementary Table S2.

Supplementary Figure S5. (a) graphical depiction of the reaction catalysed by Dicer. The apical loop of re-miR-155 is removed following cleavage at the two sites indicated by yellow triangles. The nucleotide sequence and predicted secondary structure of pre-miR-155 and miR-155/miR-155* are shown; (b) plot of the compound chemical shift changes, Δδ, recorded when TRBP-D12 is mixed with pre-miR-155 (purple) or miR-155/miR-155* (black). The location of domain boundaries, secondary structure elements and the 3 canonical dsRBD sites implicated in dsRNA binding are shown. (c) site-by-site comparison of the (^{1}H,^{15}N) chemical shift of a residue in the single domain and the corresponding residue in TRBP-D12. Circles denote (^{15}N) chemical shifts and

squares (^{1}H) chemical shifts. The points corresponding to the large outliers are annotated in grey. Rmsd values for ^{1}H and ^{15}N chemical shifts are provided.

Supplementary Figure S6.
3D models of the interaction of dsRBDs from TRBP with pre-miR-155 (left) and miR-155/miR-155* (right). The dsRNA is coloured grey and shown as a surface representation. The 4 dsRBD molecules are coloured in different shades of blue or purple and shown either as surface (top) or cartoon (bottom) representations. The 3 canonical dsRBD interaction sites are indicated in the bottom left-hand most figure.

Supplementary Figure S1

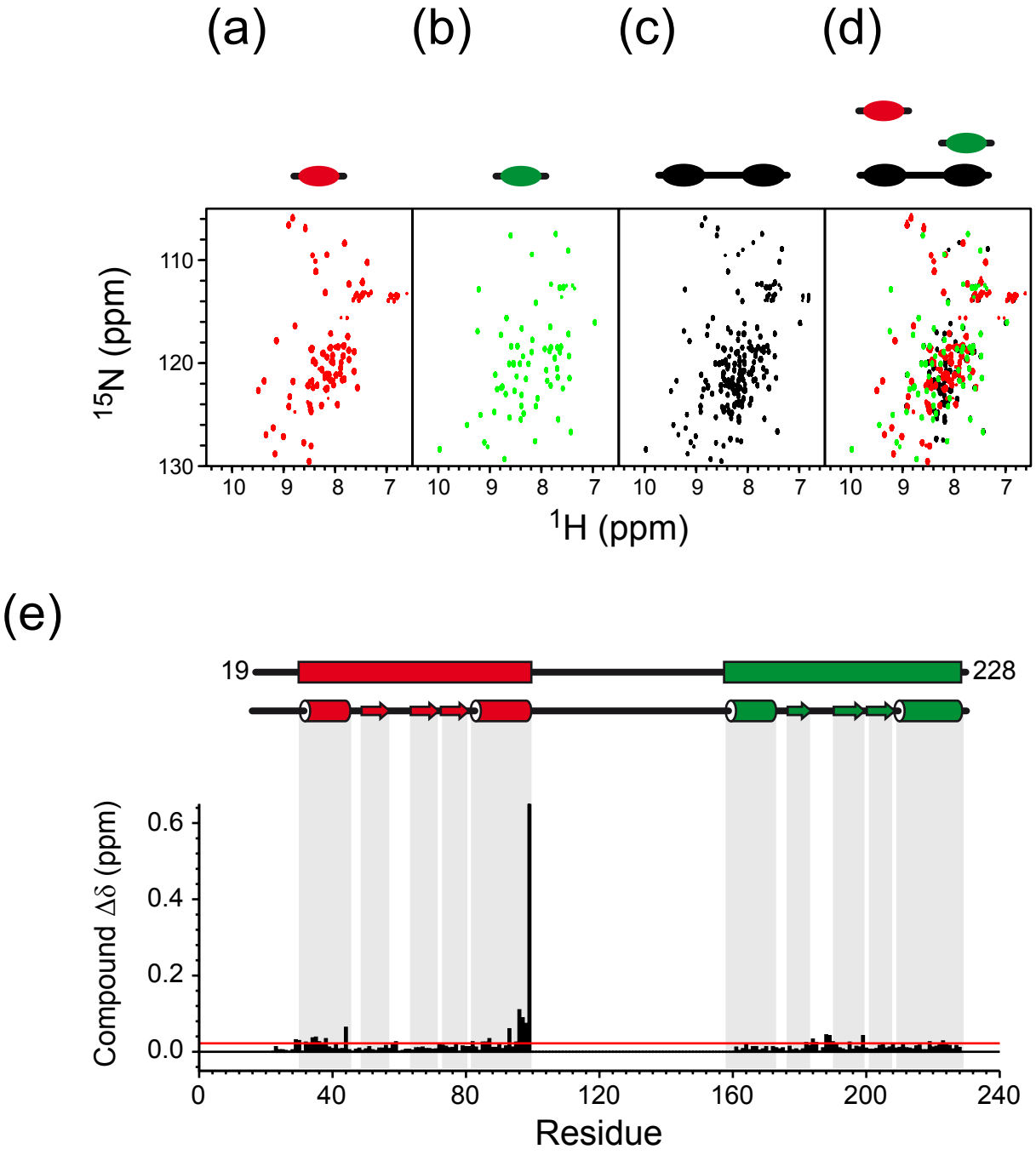

Supplementary Figure S2

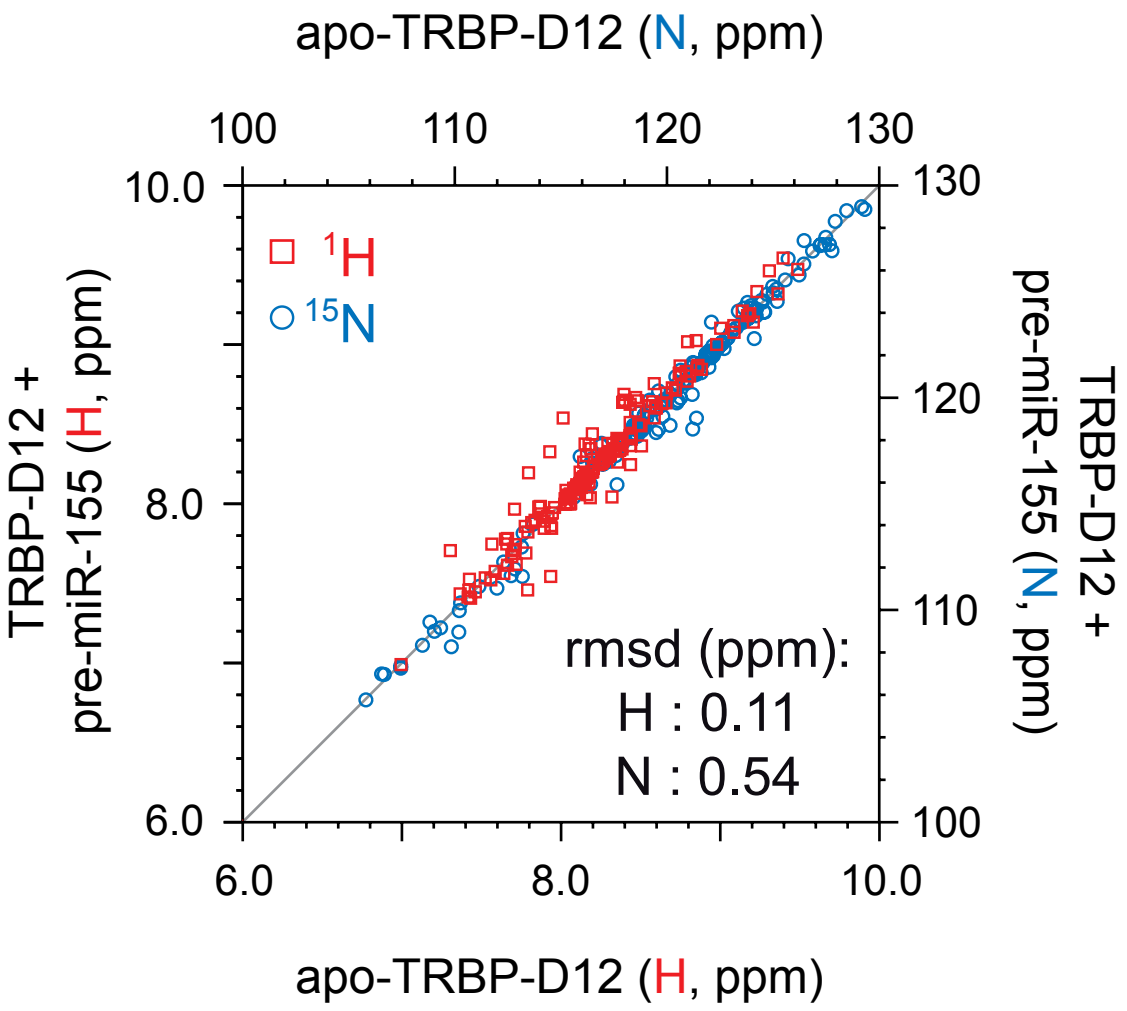

Supplementary Figure S3

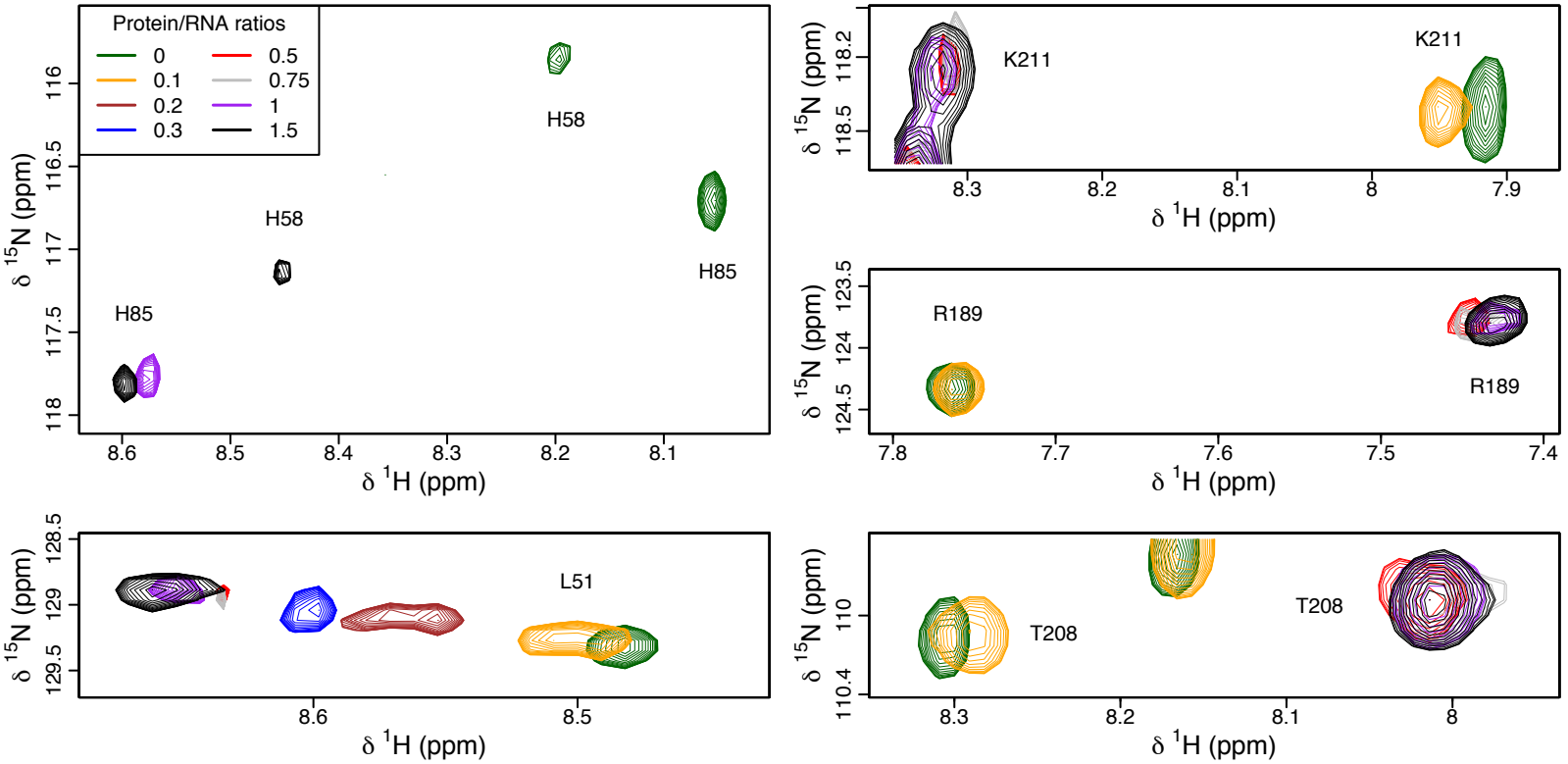

Supplementary Figure S4

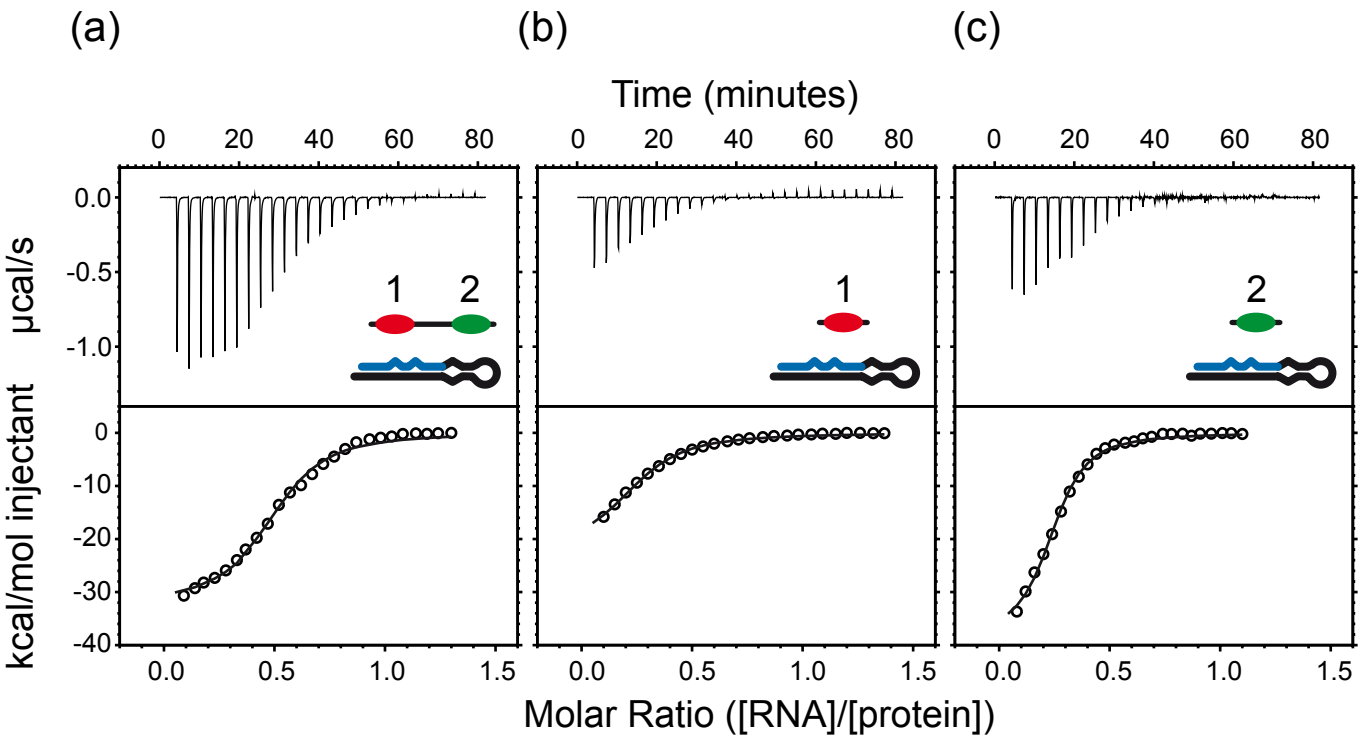

Supplementary Figure S5

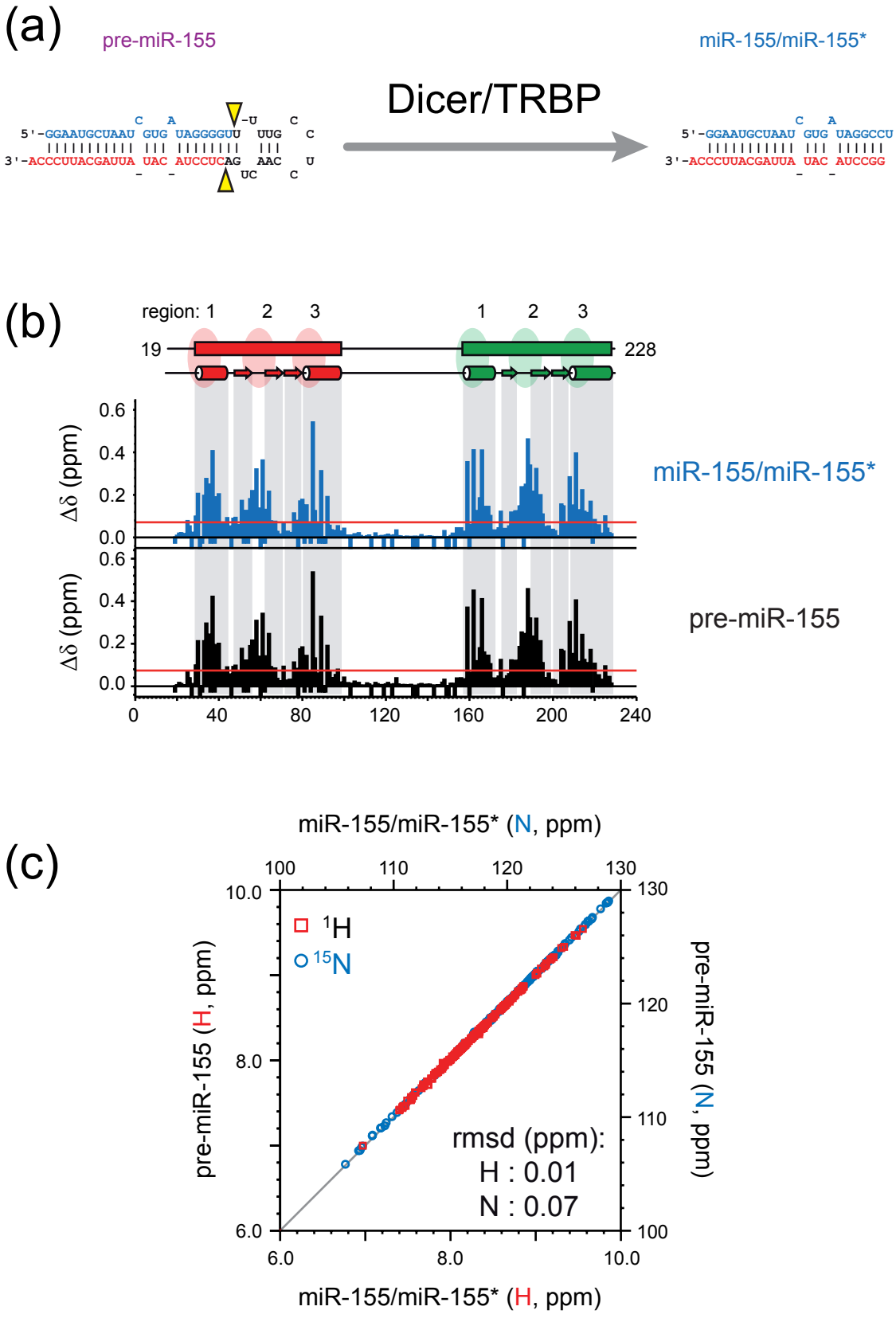

Supplementary Figure S6

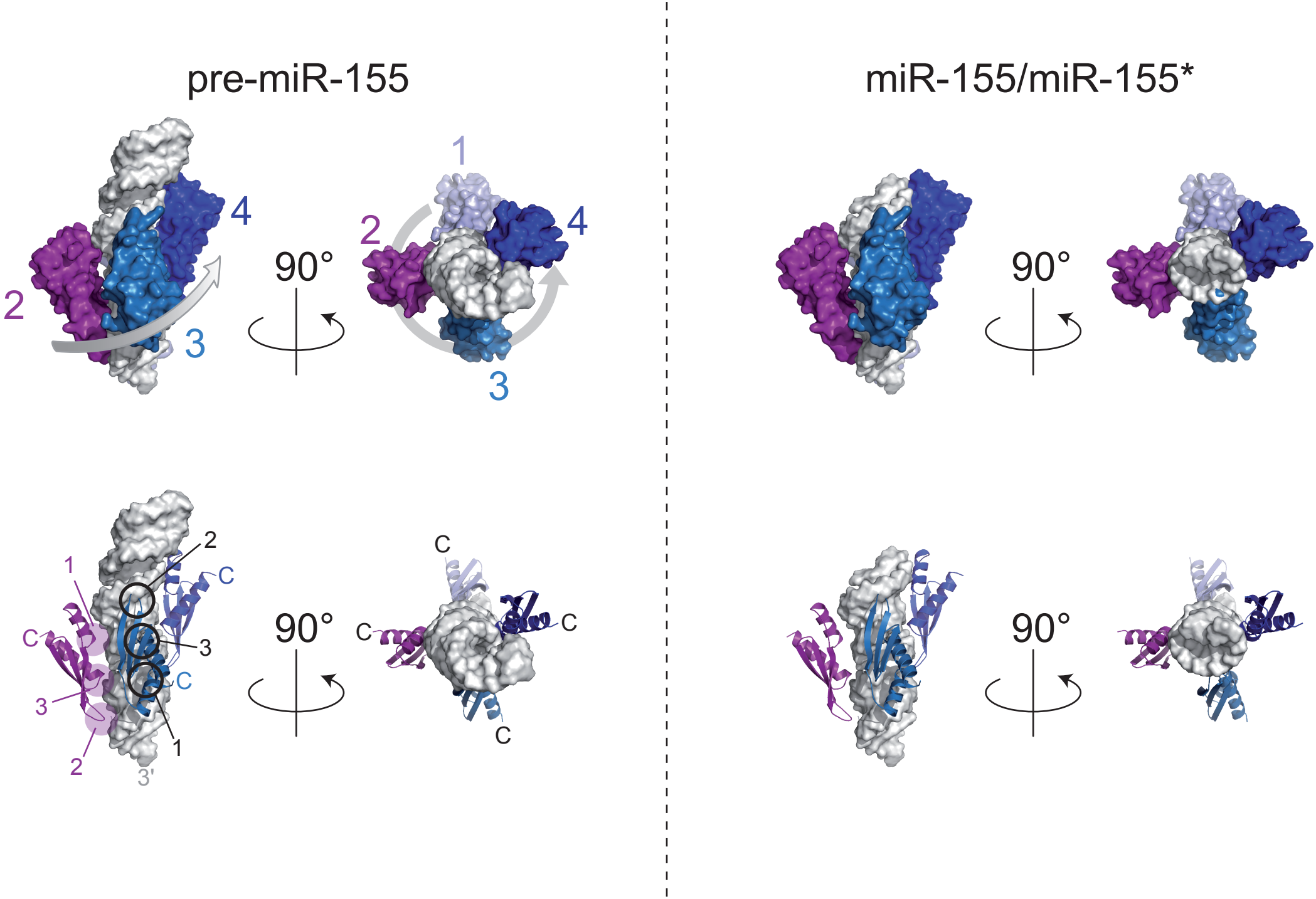

Supplementary Table 1 – Summary of svAUC data

	Experimental values					Calculated values							
Sample	s_{exp} **(S)**	M_b **(kDa)**	$\frac{A_{280}}{A_{260}}$	$\frac{\Delta J}{A_{280}}$	$\frac{\Delta J}{A_{260}}$	**Protein:RNA**	M_{calc} **(kDa)**	$\bar{v}$ **(mL/g)**	s_{calc} **(S)**	$M_{b,calc}$ **(kDa)**	$\frac{A_{280}}{A_{260}}$	$\frac{\Delta J}{A_{280}}$	$\frac{\Delta J}{A_{260}}$
TRBP-D12	2.1 (0.1)	5.7	1.73	5.7	9.9	1:0	22.3	0.74	2.1	5.7			
pre-miR-155	4.4 (0.2)	9.1	0.46	0.3	0.14	0:1	19.4	0.508	4.3	9.2			
Complex	5.9 (0.1)	18.3	0.49	0.8	0.41	1:1	41.9	0.63	4.9 - 5.5	14.9	0.47	0.53	0.25
						2:1	61.5	0.67	5.7 - 6.4	20.6	0.49	0.75	0.37
						1:2	64.2	0.59	7.0 - 7.8	24.0	0.47	0.42	0.20

s_{exp}, experimental sedimentation coefficient with standard deviation in parentheses; M_b, experimental buoyant mass determined with the non-interacting species analysis; A_{280} and A_{260}, absorbance at 280 nm and 260 nm, respectively; ΔJ, interference fringe shift; M_{calc}, $\bar{v}$ and $M_{b,calc}$, mass, partial specific volume and buoyant mass predicted from molecular composition; lower and upper s_{calc} limits for the TRBP-D12/pre-miR-155 complex were calculated using frictional coefficients of 1.4 (values calculated for free TRBP-D12 and free pre-miR-155) or 1.25 (corresponding to globular shape), respectively. The ratios for A_{280}, A_{260} and ΔJ are calculated using the experimentally determined values for TRBP-D12 and pre-miR-155.

Supplementary Table 2 – Summary of ITC results

	Syringe	Cell		K_d (µM)	*N*		ΔH (kcal mol^{-1})		ΔS (cal mol^{-1} K^{-1})
1	pre-miR-155	TRBP-D1		15.5 (0.8)	3.9 (0.2)		-6.0 (0.2)		1.9 (0.2)
2	pre-miR-155	TRBP-D2		3.7 (0.5)	4.1 (0.1)		-9.4 (0.2)		-6.8 (0.2)
3	pre-miR-155	TRBP-D12		3.4 (0.5)	2.0 (0.1)		-16.1 (0.3)		-28.8 (0.3)
4	TRBP-D12	pre-miR-155	1	0.5 (0.03)	n/a	1	-17.7 (0.1)	1	-30.5 (0.2)
			2	6.2 (0.2)	n/a	2	-8.3 (0.1)	2	-4.2 (0.3)
5	TRBP-D12	miR-155/miR155*	1	1.0 (0.7)	n/a	1	-20. 6 (0.2)	1	-41.9 (0.1)
			2	5.7 (0.3)	n/a	2	-2.3 (0.2)	2	16.3 (0.6)

The values given correspond to the combined average (and standard deviation) of the fitting parameters from a minimum of two experiments. **ROWS 1-3**: The binding isotherms resulting from the titration of pre-miR-155 into different TRBP constructs were evaluated using a single site model where *N* refers to the stoichiometry. The standard deviations associated with the reported K_d, ΔH and ΔS values were derived from experimental repetition (n ≥ 2). **ROWS 4 and 5**: The binding isotherm resulting from the titration of TRBP-D12 into different RNA samples was evaluated using a 2-site sequential binding model. $K_{d,i}$, ΔH_i and ΔS_i values are given for each binding event (i = 1 or 2). Each experiment was repeated twice. The standard deviation for each fitted parameter is indicated in parenthesis and was determined by running 100 Monte Carlo simulations of each pair of ITC curves followed by a global fitting of each pair of experiments.